# Carbide Transformations during Aging of Wear-Resistant Cobalt Alloys

S. HAMAR-THIBAULT, M. DURAND-CHARRE, and B. ANDRIES

Wear-resistant cobalt-based alloys were thermally aged for 30, 300, and 1000 hours at 650 °C and 850 °C in vacuum sealed tubes of silica. Unidirectional solidification was used to promote coarser structures easier to investigate. The precipitates were characterized by scanning and transmission electron microscopy, X-ray diffraction, and microprobe analysis. During aging secondary $M_{23}C_6$ transforms into $M_6C$. Concomitantly, the primary carbides undergo internal transformation from $M_7C_3$ to $M_6C$, and $M_6C$ loses carbon and becomes $M_{12}C$. Three main findings are reported: (1) a correlation between the nature of precipitates and the chemical segregations, (2) modification of the composition, the morphology, and the crystallographic structure of the carbides, and (3) in these alloys $M_{23}C_6$ is only an intermediate phase thermodynamically unstable.

## I. INTRODUCTION

COBALT alloys are used as wear-resistant materials for hardfacing. Their good resistance to abrasion is due to the presence of hard carbide precipitates. The presence of cobalt improves high temperature properties and resistance to various corrosive agents. In previous work[1] it was shown how the tungsten and silicon content may influence the nature and composition of carbides which appear during solidification.

The purpose of the present paper is to examine the behavior of such alloys when aged for a long time in the temperature range 650 °C to 850 °C. The composition of the alloys selected for the investigation is close to the commercial composition Stellugine 778. So, with regard to phase equilibria, they can be studied by referring to the phase diagrams published for the following systems: Co-Cr-C,[2,3] Co-W-C,[4] Co-Cr-C-W, or Mo.[5,6] The phases expected are an austenitic $\gamma$ matrix, $M_7C_3$, $M_{23}C_6$, and $M_6C$ type carbides, and, depending on temperature, some hexagonal-close-packed cobalt ($\epsilon$). Besides the phases appearing during the solidification process, secondary carbide precipitation occurs. These precipitates coarsen and their crystal structure is altered by aging. So one of the purposes of our study is to determine to what extent these modifications occur and subsequently influence the mechanical properties of the alloy.

Thermal aging was performed at two temperatures, 650 and 850 °C (corresponding to the normal temperature range of application): 850 °C is the temperature of ready secondary precipitation, and aging at 650 °C allows cobalt transformation ($\gamma \rightarrow \epsilon$) to occur. Annealing was carried out for 1000 hours. After this time, homogenization of the matrix is almost totally achieved and nothing else occurs, other than coarsening of the precipitates.

## II. EXPERIMENTAL PROCEDURE

The alloys were prepared by "Alliages Frittés S. A.". Four compositions were studied. The nominal compositions of the alloys investigated are indicated in Table I. They include two commercial compositions I and III. Number II has the composition of a three-phase eutectic as determined in a previous study.[1] Numbers III and IV have the same composition except for nickel content, in order to establish the effect of cobalt substitution.

The specimens were sealed in evacuated tubes of silica and annealed for 30, 300, and 1000 hours at 850 °C and for 30 hours at 650 °C. Such annealings were performed on two kinds of microstructures, as-cast or undirectionally solidified. These latter exhibited a coarser structure, facilitating microprobe analysis. The microstructure was examined by optical microscopy on samples etched in Murakami's reagent. Scanning electron microscopy was performed on samples with a slightly anodically dissolved matrix. More accurate observations were carried out by transmission electron microscopy. Electropolishing of the thin foils and anodical dissolution were made with an electrolyte of composition: 20 ml perchloric acid, 10 ml glycerol, and 70 ml ethyl alcohol at 0 °C and 20 volts.

Identification of phases was confirmed by X-ray diffraction using filtered chromium radiation. These investigations were made on carbides extracted from the anodically dissolved matrix (HCl 5 pct solution in water). The analysis of each phase was performed with an electron microprobe (CAMECA MS 46). As-cast and annealed alloys were tested for hardness with a Vickers microhardness tester using a load of 200 g.

## III. RESULTS

### A. *Precipitation at 850 °C within the $\gamma$ Phase*

Alloy I, which has an intermediate composition, was taken as a reference to study more particularly the aging of the alloys. As-cast structures consist of an fcc matrix and an interdendritic network of eutectic carbides. The solidification process gives successively: $\gamma$ dendrites, a two-phase eutectic $\gamma$-$M_7C_3$ and a three-phase eutectic $\gamma$-$M_7C_3$-$\eta$ carbides. The electron microprobe images (Figure 1(a)) show the distribution of the phases. Within the matrix, the $M_7C_3$ carbides appear rather light since their W content is very low. On the contrary, the $\eta$ tungsten-rich carbides are

S. HAMAR-THIBAULT and M. DURAND-CHARRE are with Laboratoire de Thermodynamique et Physico-Chimie Métallurgiques – ENSEEG – Domaine Universitaire BP44, 38401 St. Martin d'Hères, France. B. ANDRIES is with Alliages Frittés S. A. 54, Avenue Rhin-Danube 38100, Grenoble, France.

Manuscript submitted August 11, 1981.


ISSN 0360-2133/82/0311-0545$00.75/0

**Table I. Chemical Composition of Materials Examined**

| Alloy | Element | W | Si | Cr | Ni | C | Co+Fe (1 Pct) |
|---|---|---|---|---|---|---|---|
| I | At. Pct | 3.54 | 2.22 | 28.01 | 20.89 | 7.52 | bal |
| | Wt Pct | 11.38 | 1.09 | 25.48 | 21.46 | 1.58 | bal |
| II | At. Pct | 3.54 | 5.37 | 26.91 | 21.54 | 7.36 | bal |
| | Wt Pct | 11.54 | 2.68 | 24.85 | 22.46 | 1.57 | bal |
| III | At. Pct | 2.7 | 1.69 | 31.49 | 1.24 | 7.91 | bal |
| | Wt Pct | 8.9 | 0.85 | 29.3 | 1.3 | 1.70 | bal |
| IV | At. Pct | 2.66 | 2.53 | 27.76 | 20.79 | 7.42 | bal |
| | Wt Pct | 8.4 | 1.27 | 25.76 | 21.57 | 1.59 | bal |

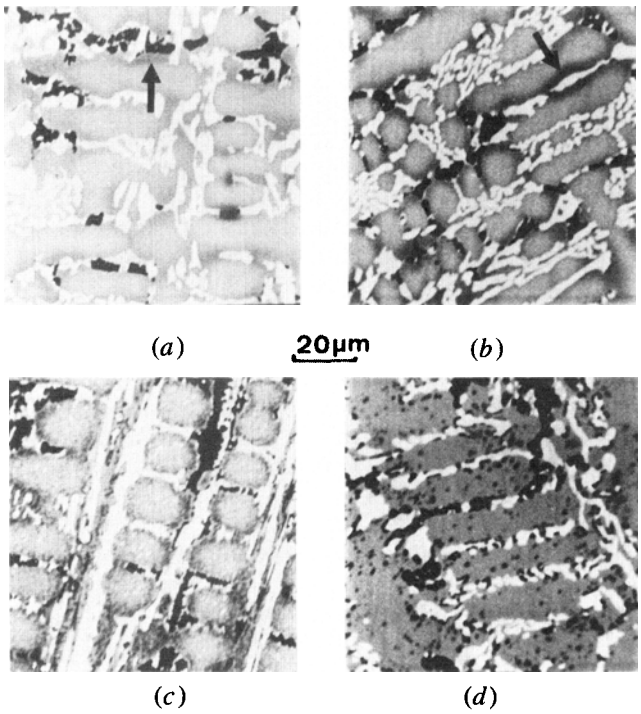


Fig. 1 — Microprobe images of sample 1: as-cast (*a*) and aged at 850 °C for 30 h (*b*), 300 h (*c*), and 1000 h (*d*) (absorbed electrons).

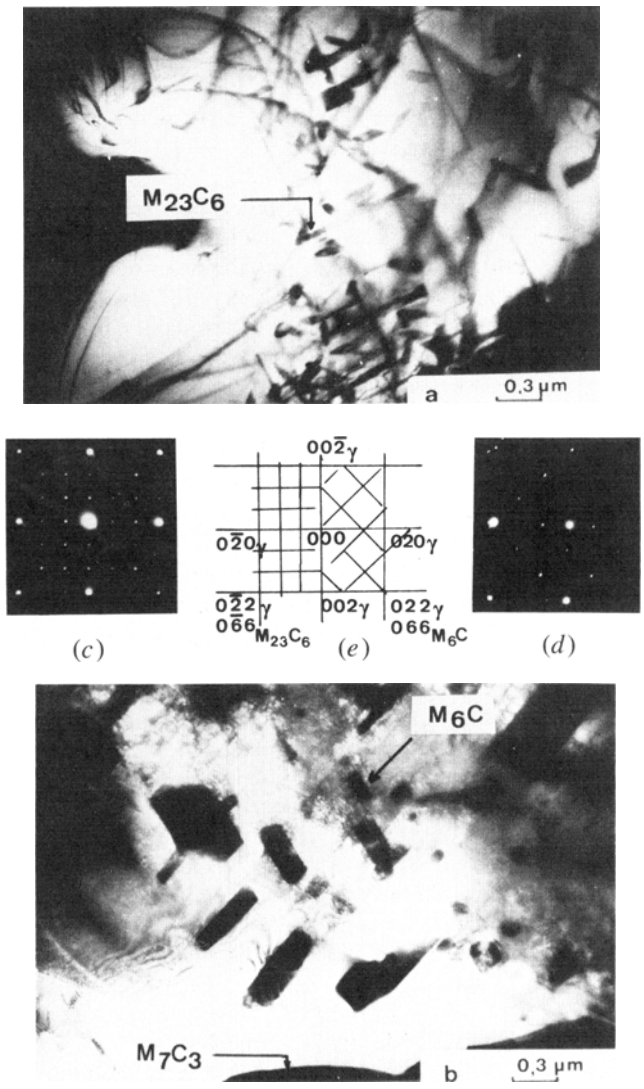


Fig. 2 — Bright field electron micrographs and diffraction patterns of sample I aged at 850 °C during 30 h (*a*), (*c*) and 300 h (*b*), (*d*). Key diagrams of the diffraction patterns (*e*).

dark. Each phase appears in its characteristic form: a spade-like shape for the $M_7C_3$ carbide and a fish-bone shape for the $\eta$ carbides.

In addition to the electron microprobe images, elemental profiles were made for tungsten and chromium. They revealed a tungsten-enriched zone at the border of the dendrites due to solidification segregation. These areas are darker than the center of the dendrite (Figure 1(a)). Furthermore, after 30 hours aging these zones appear still darker, adjacent to the $M_7C_3$ carbides, in the chromium-depleted zone (Figure 1(b)). The effect of different annealing times on the microstructure is shown in the four electron microprobe images (Figures 1(a) to (d)). Each sample was investigated in detail by transmission electron microscopy (Figure 2) and scanning microscopy (Figure 3).

After 30 hours aging at 850 °C, dark zones due to W-enriched areas have spread around the carbides. Bright field electron micrographs (Figure 2) reveal some very small plate-like coherent precipitates in the matrix grown preferentially along ⟨100⟩ directions of the matrix. The diffraction patterns show a structure of the $M_{23}C_6$ type. The orientation relationship which exists between the two lattices is:

$$\begin{cases} [001]_{M_{23}C_6} \| [001]_{\text{matrix}} \\ [010]_{M_{23}C_6} \| [010]_{\text{matrix}} \end{cases}$$

In the early stages of precipitation, the coherent particles of $M_{23}C_6$ are several nanometers long and precipitation occurs in the center of the dendrite. In the chromium-depleted zone near the eutectic carbides a precipitate-free zone has been observed.

After 300 hours and 1000 hours aging, two kinds of precipitates can be distinguished on the microprobe images (Figures 1(c) and d)): a lot of white spots of the $M_{23}C_6$ type and some black points of $M_6C$ carbides. Figure 3(a) shows the sample aged for 1000 hours as observed by scanning electron microscopy. The $M_{23}C_6$ precipitates (Figure 3(c)) appear very fine and located only within the dendritic core. On the contrary, the bulky $M_6C$ (Figure 3(b)) carbides have developed along the grain boundary in the previous

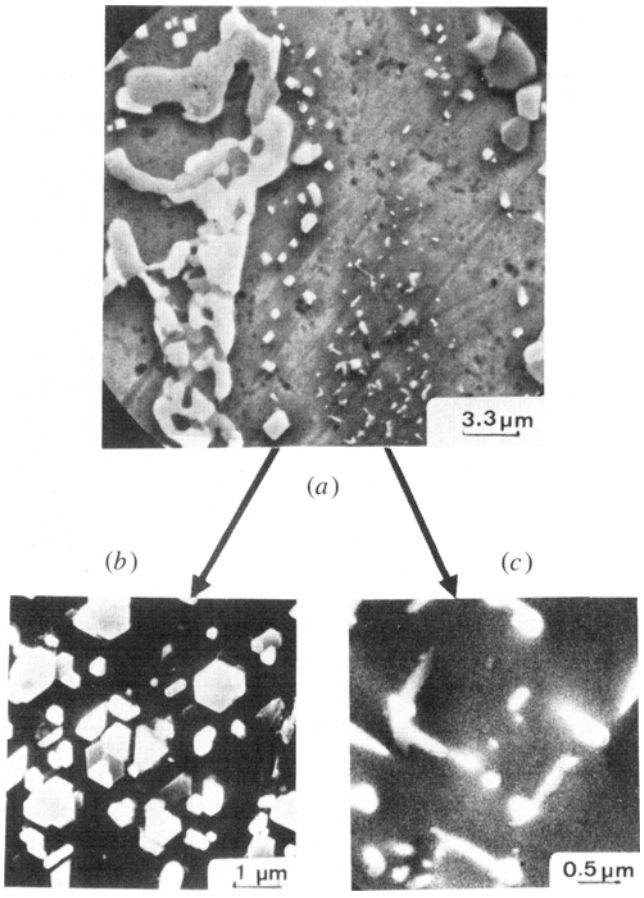


Fig. 3—Scanning electron micrographs of sample I. (*a*) Homogeneous precipitation of coherent carbides after 1000 h at 850 °C, (*b*) morphology of $M_6C$, near the boundary of the grain, and (*c*) morphology of $M_{23}C_6$, in the center of the grain.

precipitate-free zone (Figure 3(a)). So two kinetic processes may be noted: the $M_{23}C_6$ carbides grow in the early stages and remain in the form of elongated, very fine, precipitates. It takes longer for the $M_6C$ carbides to be observed. Nevertheless, once nucleated they grow more rapidly. Table II presents observations concerning the secondary carbides and illustrates their different behaviors. During annealing the $M_7C_3$ carbides undergo incomplete transformation, evident in the modification of volume fraction, chemical composition, and the lattice parameters. It can be noted that some $\eta$ carbides have grown epitaxially with the $M_7C_3$ carbides.

The orientation relationship and related lattice misfits are reported in Table III. The variation of the lattice parameter for the $\eta$ carbides is presented in Figure 4 as a function of W content. This latter parameter is significantly reduced for sample I and less so for sample II. This variation may be related to variations in composition. Besides the crystallographic transformation of the $\eta$ carbides, variations of their composition were also observed (Table IV). The analysis shows a considerable change in carbon content. The $\eta$ carbides have a composition which corresponds to a mean formula: $(Co, Ni, Si)_{2.8}$ $(Cr, W)_{3.2}C$. After annealing, the carbon content has fallen to a low level and the composition can vary widely from $M_{16}C$ to $M_{20}C$. For alloy IV, the

**Table II. Evolution of the Secondary Carbide Size on Aging at 850 °C**

| | 30 Hours | 300 Hours | 1000 Hours |
|---|---|---|---|
| $M_{23}C_6$ | Plate-like | Plate-like<br>600 nm length<br>10 nm wide | Plate-like<br>≃1500 nm length |
| $M_6C$ | — | Cubic shape<br>200 to 500 nm | Cubic shape<br>1 to 2 $\mu$m |

**Table III. Summary of Lattice Misfit and Orientation Relationships between $M_7C_3$ and $M_6C$ from Inoue and Masumoto[14] and Our Results**

| Orientation Relationship | Lattice Misfit $(d_1-d_2)/d_1$ | Orientation Relationship | Lattice Misfit |
|---|---|---|---|
| $(1\bar{1}00)_{M_7C_3}\|\|(111)_{M_6C}$ | 0.01 | $(1100)_{M_7C_3}\|\|(11\bar{1})_{M_6C}$ | 0.01 |
| $(0001)_{M_7C_3}\|\|(\bar{1}2\bar{1})_{M_6C}$ | 0.04 | $(10\bar{1}0)_{M_7C_3}\|\|(11\bar{1})_{M_6C}$ | 0.01 |
| $(11\bar{2}0)_{M_7C_3}\|\|(10\bar{1})_{M_6C}$ | 0.07 | $(0001)_{M_7C_3}\|\|(\bar{1}10)_{M_6C}$ | 0.13 |
| from Inoue and Masumoto | | Our results | |

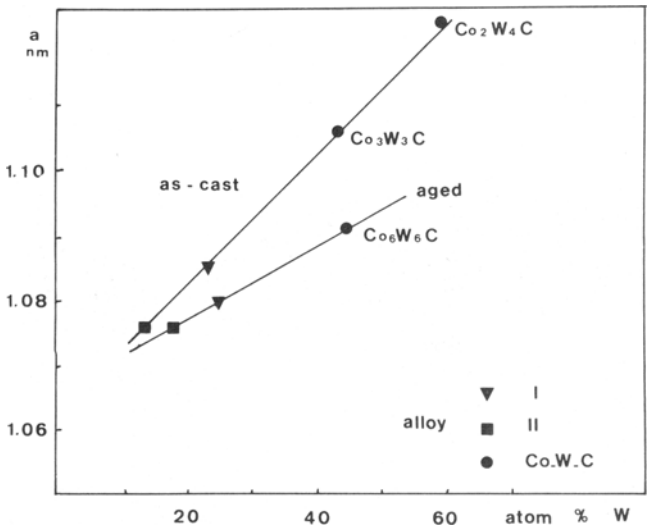


Fig. 4—Lattice parameters of $\eta$ carbides as a function of W content for as-cast alloys and alloys I and II annealed for 1000 h at 850 °C. The lattice parameters of known $\eta$ carbides is also reported ($Co_2W_4C$, $Co_3W_3C$, and $Co_6W_6C$).

composition of $\eta$ after aging could not be measured because of the very small size of the particles. This loss of carbon is consistent with the evolution of carbides reported by Sims and Hagel.[7] It is also worth noting that the amount of precipitates increases even though the amount of carbon in the carbides decreases. In spite of indications given by Johansson and Uhrenius,[8] the W content in the $\eta$ carbides evidences no significant variation. Moreover, the chemical composition of $M_7C_3$ does not change significantly; there is only a slight loss of carbon.

### B. *Aging at 650 °C*

After aging at 650 °C for 30 hours, sample I presents the following structure:

Table IV. Composition of the $\eta$ Carbides As-Cast and after Aging at 850 °C for 1000 Hours. $\eta$ Carbides Are Too Small to be Analyzed in Sample IV and in Aged Sample III. The Composition Is Given in At. Pct.

| | | Si | W | Cr | Co | Ni | C | |
|---|---|---|---|---|---|---|---|---|
| I | As-cast | 7.1 | 22.9 | 22.5 | 21.3 | 12.05 | 14.0 | $(Co\ Ni\ Si)_{2.8}(Cr\ W)_{3.2}\ C$ |
| | Aged | 9 | 24.8 | 25.2 | 20.8 | 13.2 | 7.0 | $(Co\ Ni\ Si)_{7.4}(Cr\ W)_{8.4}\ C$ |
| II | As-cast | 12.9 | 15.9 | 27.1 | 17.6 | 14.7 | 11.7 | $(Co\ Ni\ Si)_{3.8}(Cr\ W)_{3.6}\ C$ |
| | Aged | 14.5 | 17.0 | 30.2 | 19.1 | 15.7 | 4.5 | $(Co\ Ni\ Si)_{10.2}(Cr\ W)_{10.2}\ C$ |
| III | As-cast | 6.3 | 21.5 | 23.5 | 31.3 | 0.7 | 16.6 | $(Co\ Ni\ Si)_{2.4}(Cr\ W)_{2.7}\ C$ |

1. No precipitate inside the matrix.
2. A nonhomogeneous distribution of dislocations (Figure 5(a)).

On the other hand, eutectic sample II shows a high density of stacking faults around the primary particles (Figure 5(b)) and some tendency to form the hcp ($\epsilon$) Co phase.

### C. *Influence of Nickel*

Alloys I and III (the latter having a very low nickel content) behave similarly during aging: precipitation occurs in two stages: first plate-like $M_{23}C_6$, then bulky shaped $M_6C$, the matrix remaining predominantly fcc. Figure 6 shows the microstructure of sample III before and after aging. Some precipitates appear in the form of blocks (single arrow) and others as needles (double arrow). We have never observed such long needles in other alloys. As regards composition, no difference could be detected between the two shapes. Their composition is very similar to that of the $\eta$ carbides. On the contrary, with sample I there are very few $M_{23}C$ precipitates. In addition we observe (Figure 7(a)) a high density of stacking faults, and some $\varepsilon$ cobalt phase. The diffraction pattern (Figures 7(d) and (e)) shows unambiguously some spots of hcp $\varepsilon$ cobalt together with those of a $\gamma$ matrix (Figure 7(b)). Streaked reflections are associated with the very small size of the hcp lamellae (Figure 7(c)) along the plane (111). These observations are in agreement with the experiments of Beaven, Swann, and West.[9]

Nickel stabilizes the fcc matrix, as reported by Sims.[7] In this respect, nickel counteracts the tendency of chromium and tungsten to form excessive stacking faults.

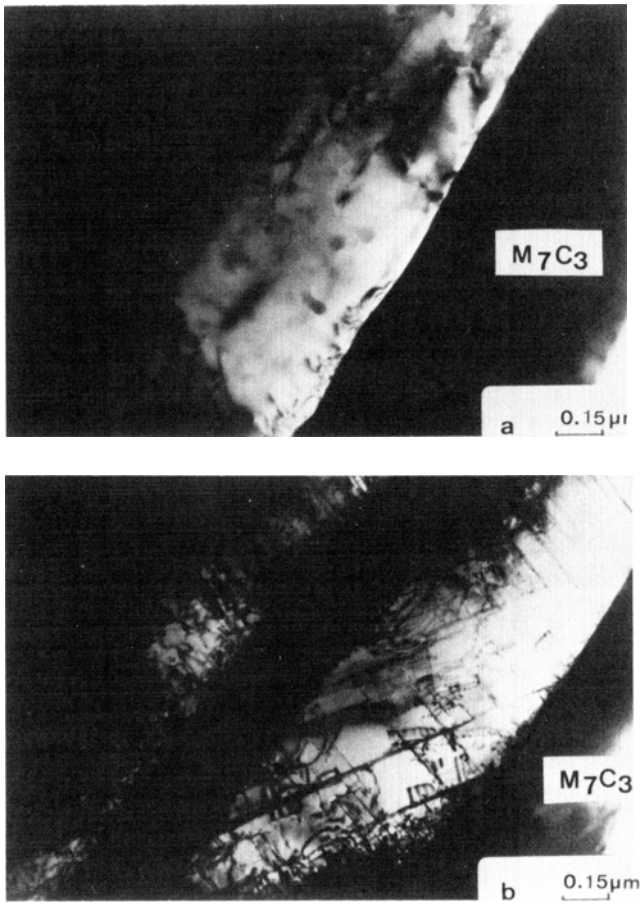


Fig. 5 — Some bright field electron micrographs of sample I (*a*) and II (*b*) aged 30 h at 650 °C.

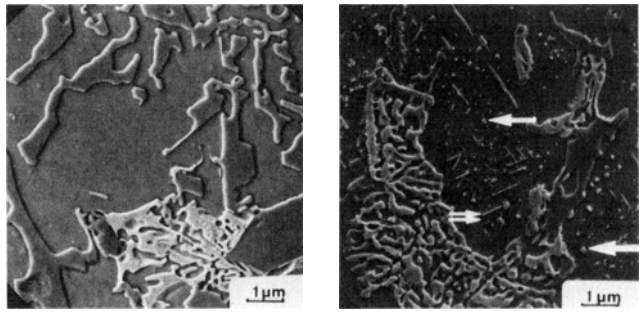


(*a*) (*b*)

Fig. 6 — Scanning electron micrographs before (*a*) and after aging (*b*) at 850 °C for 1000 h for sample III.

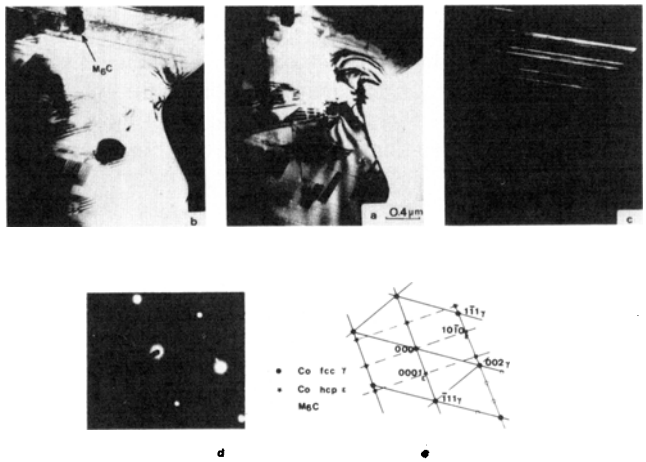


Fig. 7 — Electron micrograph of Sample III: (*a*) Bright field, (*b*), (*c*) dark fields on a Co fcc spot and Co hcp spot, and (*d*), (*e*) diffraction pattern and key diagram.

D. *Hardness Measurements*

The microhardness of the as-cast materials varied little with aging time. It is about 450 $HV_{200}$ for sample I. After aging the matrix did not harden significantly with precipitation and measured 450 to 500 HV. This very small variation is in good agreement with the results of Beaven *et al.*[9] However, for sample III having an almost eutectic microstructure, the microhardness of the matrix falls to 300 to 350 HV due to lack of precipitates.

## IV. DISCUSSION

As shown previously (Figures 1 to 3), $M_6C$ precipitates near the border of the grain, where the chemical content of W is increased by solidification segregation. We suggest in accordance with Johansson and Uhrenius[8] the following reaction:

matrix (high W) + carbon→matrix (low W) + $M_6C$

In fact, we did not detect a noticeable loss of W from the $\eta$ carbides (Table IV). The tungsten necessary to build up these carbides is removed from the matrix. On the contrary, the carbon content of the different solidification carbides decreases after aging, providing carbon is able to produce new precipitates of $M_{12}C$. During aging, $M_7C_3$ decomposes and is replaced by $M_6C$, as exhibited in Figure 3(a), while the composition of the latter evolves to $M_{12}C$.

As the literature leads us to expect,[7,12] $M_{23}C_6$ nucleates and grows during aging. Its W content can increase up to the formula $Cr_{21}W_2C_6$ proposed by Goldschmidt.[10] However, our observations show that after 1000 hours aging $M_{23}C_6$ is almost completely transformed into $M_6C$. The isothermal 1050 °C section of the phase diagram given by Knotek and Seifahrt[5] for the systems Co-Cr-W-1 pct C, Co-Cr-W-1 pct C-1 pct Si are reported in Figure 8. Comparing our values for the composition of the matrix (Table V) with this section, it appears that $M_{23}C_6$ should not be an equilibrium phase in the presence of silicon. In fact, this element enlarges the three-phase domain $\gamma$, $M_7C_3$, $\eta$ (A on Figure 8), and shifts the four-phase domains $\gamma$, $M_7C_3$, $\eta$, $M_{23}C_6$ (from $B_0$ to $B_S$ on Figure 8).

The presence of $M_{23}C_6$ must be explained other than by interfacial thermodynamic considerations. It is generally admitted that a good match across the interface plane results in a low interfacial energy. The lattice parameter of the matrix is almost one third that of $M_{23}C_6$. Additions of W or Mo increase the lattice parameter[16] from 1.065 to 1.071 nm when the Mo content increases from 0 to two atoms per formula. Nevertheless, the misfit remains tiny, as evident from the precise overlapping of the spots in the diffraction patterns (Figure 2). This strong coherency promotes ready nucleation of $M_{23}C_6$, though it is not a thermodynamically stable phase. With regard to the $\eta$ carbides (lattice parameter $\simeq$1.084 nm) the misfit reaches two pct and nucleation is more difficult; consequently, precipitation takes place later. Moreover, $M_6C$ carbide growth requires diffusion of W, and tungsten diffusivity is very low.

Apart from the problem of nucleation in the matrix, prolonged aging gives rise to transformations of the carbides which are well known in steels[13,14,15] and superalloys.[7]

The orientation relationships we have found between the different kinds of carbides are to be compared with the results obtained for steels.[14] Table III sums up all the results. The two orientation relationships, ours and that of Inoue and Masumoto,[14] differ by a 30 deg rotation around the [111] direction, and the pair of parallel planes is the same in both cases. According to their result for relative orientation Inoue and Masumoto[14] deduce that the small value of misfit favors the transformation. The orientation we observed led to a misfit of the same order of magnitude, and the same conclusion can be put forward. In the relative orientation we observe, two pairs of dense planes are parallel. Then the transformation may be induced by the internal faults which lie precisely on the $(1\bar{1}00)$ and $(\bar{1}010)$ planes.[14]

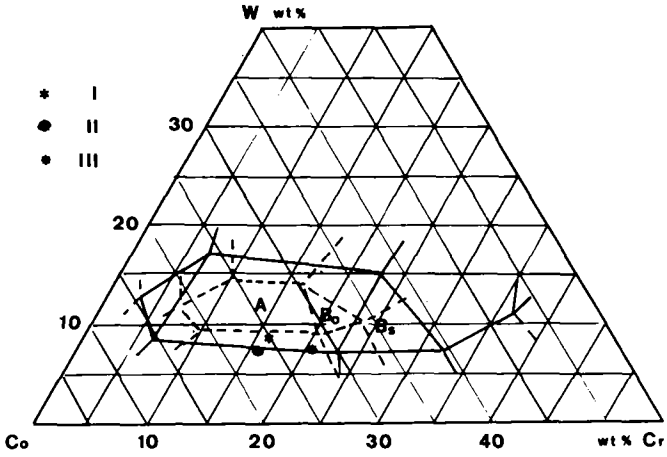


Fig. 8—Isothermal section of the phase diagram at 1050 °C for system CoCrW 1 pct C (dotted line) and CoCrW 1 pct C-1 pct Si (continuous line), from Knotek and Seifahrt.[5] A is the three phase domain $\gamma + \eta + M_7C_3$. $B_s$ and $B_0$ are the four phase domains ($\gamma + \eta + M_7C_3 + M_{23}C_6$) and are related to the diagrams with and without silicon.

**Table V. Composition (At. Pct) of the Matrix of the Four Alloys. Carbon Content Was Not Detectable**

| | Si | W | Cr | Co | Ni | C |
|---|---|---|---|---|---|---|
| I | 2.4 | 2.7 | 22.3 | 44.7 | 27.7 | — |
| II | 5.7 | 1.9 | 20.4 | 44.7 | 27.3 | — |
| III | 2.5 | 1.9 | 26.2 | 64.5 | 1.9 | — |
| IV | 2.1 | 2.1 | 21.3 | 47.0 | 27.2 | — |

## V. CONCLUSION

Our investigations of the aging of wear-resistant alloys led to three main findings:

1. There is a strong correlation between the nature of the precipitates and local chemical composition.
2. During aging the carbides undergo internal transformations. $M_7C_3$ transforms during aging into $\eta$ carbides, whose composition changes from $M_6C$ to $M_{12}C$.
3. Strict coherency occurs and promotes the nucleation of intermediate precipitates of $M_{23}C_6$.

However, precipitation has little influence upon hardness after aging.

## REFERENCES


1. M. Durand-Charre, S. Hamar-Thibault, and B. Andries: *Mém. Sci. Rev. Mét.*, 1981, vol. 78, pp. 321-28.
2. W. Koster and F. Sperner: *Archiv für das Eisenhüttenwesen*, 1955, vol. 26, pp. 555-61.
3. K. Löbl and H. Tüma: *Mém. Sci. Rev. Mét.*, 1970, vol. 67, pp. 11-16.
4. C. B. Pollok and H. H. Stadelmaier: *Metall. Trans.*, 1970, vol. 1, pp. 767-70.
5. O. Knotek and H. Seifahrt: *Archiv für das Eisenhüttenwesen*, 1968, vol. 39, pp. 869-75.
6. J. B. Vander Sande, J. R. Coke, and J. Wulff: *Metall. Trans. A*, 1976, vol. 7A, pp. 389-97.
7. C. T. Sims and W. C. Hagel: *The Superalloys*, J. Wiley, New York, NY, 1972, pp. 145-85.
8. T. Johansson and B. Uhrenius: *Metal Sc.*, 1978, vol. 12, pp. 83-94.
9. P. A. Beaven, P. R. Swann, and D. R. F. West: *J. Materials Sci.*, 1979, vol. 14, pp. 354-64.
10. H. J. Goldschmidt: *Interstitial Alloys*, Buttersworths, London, 1967, p. 104.
11. M. Durand-Charre, S. Hamar-Thibault, and F. Durand: *Z. Metallkunde*, 1980, vol. 71, pp. 802-08.
12. B. Lux and W. Bollman: *Cobalt*, 1961, vol. 12, pp. 32-38.
13. J. Beech and D. H. Warrington: *J. I. S. I.*, 1966, vol. 204, pp. 460-68.
14. A. Inoue and T. Masumoto: *Metall. Trans. A*, 1980, vol. 11A, pp. 739-47.
15. M. J. Godden and J. Beech: *J. I. S. I.*, 1970, vol. 208, pp. 168-71.
16. I. Andersson and B. O. Lundberg: *Metall. Trans. A*, 1977, vol. 8A, pp. 787-90.